Aeromechanics Analysis of a Heavy Lift Slowed-Rotor Compound Helicopter

Hyeonsoo Yeo

Aeroflightdynamics Directorate (AMRDEC)
U.S. Army Research, Development, and Engineering Command
Ames Research Center, Moffett Field, California

Wayne Johnson

Flight Vehicle Research and Technology Division
NASA Ames Research Center
Moffett Field, California

Abstract

A heavy lift slowed-rotor tandem compound helicopter was designed as a part of the NASA Heavy Lift Rotorcraft Systems Investigation. The vehicle is required to carry 120 passengers over a range of 1200 nautical miles and cruise at 350 knots at an altitude of 30,000 ft. The basic size of the helicopter was determined by the U.S. Army Aeroflightdynamics Directorate's design code RC. Then performance optimization and loads and stability analyses were conducted with the comprehensive rotorcraft analysis CAMRAD II. Blade structural design (blade inertial and structural properties) was carried out using the loading condition from CAMRAD II. Performance optimization was conducted to find the optimum twist, collective, tip speed, and taper using the comprehensive analysis. Designs were also developed for alternate missions to explore the influence of the design condition on performance.

Notation

A	rotor disk area
C_D	drag coefficient
C_f	skin friction coefficient
C_T	rotor thrust coefficient
C_W	rotor weight coefficient
D/q	airframe drag divided by dynamic pressure
L/D	aircraft effective lift-to-drag ratio
M	Mach number
M_{at}	advancing tip Mach number
P	aircraft power
P_{req}	required power
R	rotor radius
S_{wet}	wetted area
V	flight speed
V_{br}	best range flight speed
W	gross weight
W/A	disk loading
μ	advance ratio
ρ	air density
σ	solidity
HOGE	hover out of ground effect
ISA	international standard atmosphere
MCP	maximum continuous power
MRP	maximum rated power
OEI	one engine inoperative
SFC	specific fuel consumption
SHP	shaft horse power
SLS	sea level standard
SOA	state of the art
VTOL	vertical takeoff and landing

Presented at the American Helicopter Society International Vertical Lift Aircraft Design Conference, San Francisco, California, January 18-20, 2006.

Introduction

The NASA Heavy Lift Rotorcraft Systems Investigation was conducted to identify candidate configurations for a large civil VTOL transport that is technically promising and economically competitive [1]. The vehicle is required to carry 120 passengers over a range of 1200 nautical miles and cruise at 350 knots at an altitude of 30,000 ft. A large civil tandem compound (LCTC) helicopter was designed as one of the candidate configurations to meet this NASA 15-year notional capability. The rotorcraft notional capabilities and sector technology goals are in Tables 1 and 2, respectively.

The compound helicopter is one of the methods of achieving high speed capability while retaining the hover advantages of a helicopter. The compound helicopter is defined as a helicopter with both a wing and auxiliary propulsion. In general, the lifting and propulsive force capabilities of a helicopter rotor decrease with forward speed as a result of asymmetric flow conditions encountered by the rotor. The compound helicopter circumvents these limits by sharing lift between the wing and rotor as well as eliminating the need for rotor

propulsive force. To maintain low rotor drag at high speed, it is necessary to slow the rotor.

This paper presents the results of the heavy lift slowed-rotor tandem compound helicopter design investigation. It describes the approach used for developing the design. The complete design is presented together with an optimization study conducted. Designs were also developed for alternate missions to explore the influence of the design condition on performance.

Design Approach

The design process of the heavy lift slowed-rotor tandem compound helicopter is shown in Fig. 1. Rotorcraft behavior is inherently multidisciplinary and its design is fundamentally an iterative process. The basic size of the helicopter was determined by the U.S. Army Aeroflightdynamics Directorate's design code RC [2]. Then performance optimization and loads and stability analyses were conducted with the comprehensive rotorcraft analysis CAMRAD II [3]. Blade structural design (blade inertial and structural properties) was carried out using the loading condition from CAMRAD II [4]. The design process was completed when the vehicle performance, loads, and stability results did not change between iterations.

Rotorcraft sizing processes parametric equations and semi-empirical math models with designer inputs. RC iterates on the rotorcraft design (engine size, rotor diameter, gross weight, etc.) until it reaches a converged solution that meets design requirements (payload, range, etc.). During each step of the iteration cycle, RC also conducts design-critical flight and mission performance analysis. The rotor performance model in the RC sizing code was calibrated using the performance calculated by CAMRAD II, and the sizing task repeated. An estimate of the drag of the airframe was used to define the aerodynamic model for the sizing code and the comprehensive analysis. In the current analysis, the sizing code incorporated significant weight savings (relative to current technology scaled to large size) as a result of structure, drive train, and engine technology, such as new materials, new design methods, new operating procedure, etc.

CAMRAD II is an aeromechanics analysis of rotorcraft that incorporates a combination of advanced technologies, including multibody dynamics, nonlinear finite elements, and rotorcraft aerodynamics. The trim task finds the equilibrium solution for a steady state operating condition, and produces the solution for performance, loads, and vibration. The flutter task linearizes the equations about the trim solution, and produces the stability results. The aerodynamic model includes a wake analysis to calculate the rotor nonuniform induced-velocities, using rigid, prescribed, or free wake geometry. CAMRAD II has undergone extensive correlation of performance and loads measurements on helicopters [5–7]. A complete aeroelastic model was developed for the analysis of the compound helicopter.

A low weight rotor system is an important goal for the design of a heavy lift helicopter. Blade structural loads calculations were used to design composite rotor blade sections, and the resulting blade structural and inertial properties were used to repeat the loads and stability calculations. The blade cross section design/optimization procedures were developed to achieve the targeted weight reduction, while satisfying the stiffness and strength requirements.

Mission and Design Conditions

The mission is to transport 120 passengers over a range of 1200 nautical miles. The payload comprises 120 passengers at 220 lb each (190 lb + 30 lb baggage), 2 flight crew at 240 lb each and 3 cabin crew at 210 lb each. The design mission and power requirements are described in Table 3. Although the aircraft was designed to the mission defined in Table 3, hence with very little hover time (2 minutes), efficient hover and low speed capability is essential for a VTOL transport. This is reflected in the requirement for OEI hover capability. The resulting designs optimize at balanced cruise and OEI hover power [8].

Critical design conditions appropriate for civil heavy lift rotorcraft operations were defined for calculation of performance, loads, and stability. Table 4 summarizes these aeromechanics analysis conditions. The comprehensive analysis code was used to conduct the aeromechanical analysis of Table 4.

Technology Factors and Design Parameters

High speed, high altitude, and long range are required to meet the technology goals of the current investigation. The heavy lift rotorcraft must have low disk loading for good hover efficiency, and low drag for efficient cruise. The target for improvement in hover efficiency implies a disk loading of about W/A = 10 lb/ft^2. The actual disk loading of the design was determined based on minimum aircraft weight, power, and cost.

Figure 2 shows historic trends for aircraft drag. For the current heavy lift rotorcraft investigation, the target

airframe and wing drag was D/q = $1.6(W/1000)^{2/3}$. This drag level is higher than current turboprop aircraft, although about 24% lower than is customary in the helicopter industry. Consequently, good aerodynamic design practice should be sufficient to achieve the target for airframe drag. Figure 3 shows historic trends for rotor hub drag. In cruise, hub drag must be added to the airframe and wing drag of the aircraft. For this investigation, the target hub drag was D/q = $0.4(W/1000)^{2/3}$, which is less than half of current hub drag levels. Achieving this hub drag level will require advanced technology, certainly fairings but possibly also active flow control.

An assessment of engine and drive train technology was made in order to define and substantiate the sizing code models. The engine model represents what can be obtained from (or required of) a modern technology engine. A drive train concept was developed for the heavy lift rotorcraft design described here [9].

Basic parameters of the rotorcraft were chosen based on an assessment of current and future technology, as shown in Table 5. The rotor blade loading (C_W/σ = 0.141, based on gross weight and thrust-weighted solidity) was chosen based on low speed maneuverability requirements. The C_W/σ value corresponds to about an 8% improvement in maximum lift capability, compared to current technology. A relatively low hover tip speed (650 ft/sec) was used, reflecting the importance of the noise goal. The cruise tip speed was chosen to optimize the performance. Hover download value used in this study is consistent with current technology. A low wing loading (80 lb/ft^2) was chosen for good low speed maneuverability and a wide conversion speed range. The total drag (D/q/$(W/1000)^{2/3}$) was 1.9. Table 6 shows the cruise drag buildup.

Summary of Design

The heavy lift slowed-rotor compound helicopter configuration developed in this study is shown in Fig. 4. The aircraft has two main rotors in tandem configuration, a high wing, pusher propellers for cruise propulsion, and a horizontal tail. The length of the fuselage follows from the specification of the payload, and the disk loading was optimized to balance the cruise and hover power. As a result, there was no overlap of the rotors. The two rotors are separated by 90 ft horizontally and 5.8 ft vertically. The shaft incidence is 0 deg for both forward and rear rotors. The horizontal tail was sized by trim requirements rather than stability.

Table 7 shows the characteristics of the heavy lift slowed-rotor tandem compound helicopter design. Performance, loads, and stability calculations were performed for the conditions defined in Table 4. The comprehensive analysis modeled the auxiliary propulsion as forces applied to the airframe. Rotor/rotor and rotor/wing interference were accounted for using the vortex wake model. For all the calculations made in this study, an elastic blade model was used.

In hover and low speed flight, standard tandem helicopter controls, plus aircraft pitch and roll attitude, could be used to trim this aircraft. At moderate speeds, the pitch angle could be fixed and the propeller thrust trimmed instead. Even at low speeds, the lateral stick would be connected to the ailerons, and the longitudinal stick to the elevator.

Load factor sweep was conducted at 80 knots, sea level, 650 ft/sec tip speed. The turn rate was increased to achieve a load factor of up to 1.5g. The analysis was conducted using nonuniform inflow with a free wake geometry. For the load factor sweep (to obtain blade loads), the mean propeller thrust was fixed at the aircraft drag value, and the pilot's controls (collective, and longitudinal and lateral cyclic pitch), aircraft pitch and roll attitude, aircraft lateral stick (connected to ailerons), and pedal (connected to differential propeller thrust) were used to trim the aircraft. In addition, rotor flapping was trimmed to zero (for load control). Thus, there were 10 trim variables for the load factor sweep.

In cruise, the aircraft was trimmed using lateral stick to the ailerons, longitudinal stick to the elevator, pedal to differential propeller thrust; plus propeller thrust, and aircraft pitch and roll angles. Front and rear rotor collective pitch angles were set to values optimized for cruise performance (optimized rotor thrust). In addition, rotor flapping was trimmed to zero (for load control) using rotor cyclic pitch; thus there were 10 trim variables for cruise.

A hingeless rotor hub was used. To reduce mean blade lag bending moment, the hub incorporated 0.006-R torque offset. Blade structural design (blade inertial and structural properties) was performed using the blade loads for the load factor sweep. The half peak-to-peak blade flap and lag bending and torsion moment values at 50%R of the front rotor blade are shown in Fig. 5. The highest load factor used was 1.48 with the turn rate of 15 deg/sec. The blade loads for the load factor sweep were higher than those for the level flight speed sweep as shown in Fig. 6.

Figure 7 shows the calculated blade frequencies, at a collective pitch angle of 10 deg. At helicopter-mode tip speeds, the lag frequency was above 6/rev and the torsion frequency about 7.5/rev. Rotor stability calculation was

conducted in hover and forward flight condition. Figure 8 shows damping ratio as a function of thrust at sea level standard condition. No stability issues were observed up to C_T/σ of 0.2, although the damping ratio of the 2nd flap mode was significantly reduced for C_T/σ of larger than 0.18. Figure 9 shows stability calculations in level flight for 30K ISA condition. No stability issues were observed up to 500 knots.

Performance results from the comprehensive analysis are shown in Figs. 10 and 11. These results are for the state-of-the-art rotor airfoils. The final design was obtained using an optimum twist of 0 deg inboard (0.0R to 0.5R) and -12 deg outboard (0.5R to 1.0R), an optimum collective angle of -2 deg, and a taper of 0.8 (tip/root chord). These performance optimization results will be further discussed in the next section. The hover figure of merit of an isolated rotor is calculated for 5k/ISA+20^{o}C condition with 650 ft/sec tip speed. The results are shown in Figure 10. The calculation was conducted using nonuniform inflow with a free wake geometry. The figure of merit increases as the thrust increases up to around $C_T/\sigma = 0.18$, and then decreases. The figure of merit is around 0.73 at the design thrust ($C_T/\sigma = 0.149$). Figure 11 shows the aircraft lift-to-drag ratio at 30,000 ft. The calculation was conducted using nonuniform inflow with a prescribed wake geometry. Rotor/rotor and rotor/wing interference were included in the comprehensive analysis model. The speed was varied from 250 to 450 knots; with the rotor tip speed decreased from hover to cruise speed (350 knots) to maintain $M_{at} = 0.8$ and then 205 ft/sec tip speed was maintained up to 450 knots. The rotor performance in cruise is presented in terms of aircraft L/D=WV/P, calculated without accessory or other losses, and using a propeller efficiency of 0.86 (from the sizing code). The aircraft lift-to-drag ratio decreases as speed goes up. At the design cruise speed, the aircraft lift-to-drag ratio is 10.14.

The maximum hover figure of merit of the compound tandem rotor occurs at around $C_T/\sigma = 0.17$ (Fig. 10), which is high compared with many conventional helicopter rotors. The figure of merit for a conventional articulated rotor was calculated and compared with that of the compound tandem rotor, as shown in Fig. 12. The conventional rotor had 7 blades, existing airfoils, and typical solidity, twist, tip speed. The maximum figure of merit of the conventional rotor occurred at low blade loading and the figure of merit value decreased as the blade loading increased. A parametric study was conducted to examine the differences in the figure of merit trend. The parameters investigated in this study are twist, taper, tip speed, and airfoils. The effects of those parameters on the prediction of hover figure of merit were examined by replacing the compound tandem rotor quantities with the conventional rotor quantities. Figure 12 shows the parametric study results. The twist, taper, and tip speed increased the figure of merit at low blade loading, but decreased it at high blade loading. The biggest influence came from the airfoil change. A significant reduction of the hover figure of merit was observed at high blade loading and the trend became similar to the conventional rotor. It appears that the state-of-the-art airfoils used for the compound tandem rotor design have a strong influence on the figure of merit trend.

Performance Optimization

This section describes performance optimization conducted with the comprehensive analysis. The blade twist was varied to optimize the rotor for hover and cruise performance. The hover condition was 5k/ISA+20^{o}C, 650 ft/sec tip speed, $C_T/\sigma = 0.149$. The cruise condition was 350 knots, 30k ISA, 205 ft/sec tip speed, 138,764 lb gross weight. The twist distribution had two linear segments, inboard (0.0R to 0.5R) and outboard (0.5R to 1.0R). Figure 13 presents the results for twist optimization. For each value of outboard twist (-15, -12, -9, -6, -3, and 0 deg), the inboard twist values are -3, 0, 3, and 6 deg. Two linear twist segments perform better than a single linear twist distribution as shown in Fig. 14. A large negative twist improves hover performance, but the zero twist gives the best cruise performance. The optimum twist of 0 deg inboard and -12 deg outboard was selected based on the hover-cruise compromise. The optimum twist shows almost same (0.3% improvement) hover figure of merit as the -9 deg linear twist case, but the aircraft L/D was 1.6% larger than that for the -9 deg linear twist case.

Collective pitch of the front and rear rotors was varied to find the optimum rotor thrust for high speed cruise. For an untwisted rotor, the best aircraft performance would be obtained with zero collective (no lift, no induced power, minimum profile power). With negative outboard twist, for improved hover performance, the optimum collective angle was -2 deg for both front and rear rotors, as shown in Fig. 15(a). The optimum collective angle resulted in the rotors carrying about 6.8% of the aircraft lift (the rotor thrust variation with collective was negative at this high advance ratio), as shown in Fig. 15(b). This optimum occurred with a small, positive shaft power to the rotors. With the rotor in autorotation (achieved using an aft tilt of the rotor) the rotor thrust was large, hence the total rotor drag larger and the aircraft L/D somewhat smaller.

The rotor advancing tip Mach number was varied from 0.7 to 0.9 to find the optimum rotor rotational speed for

high speed cruise flight, as shown in Fig. 16. To maintain low rotor drag at high speed, it is necessary to slow the rotor. The optimum cruise performance was found at M_{at} = 0.80 (for the airfoils used). Further reductions in rotor rotational speed did not improve the aircraft L/D.

The blade taper was varied as shown in Fig. 17. The taper model considered was constant thrust-weighted solidity (chord at 75%R). The aircraft L/D decreased as the taper was reduced. Although the taper of 1.0 produced the best aircraft L/D, the taper of 0.8 (tip/root chord) was selected to reduce the blade weight.

Alternate Missions

The slowed-rotor compound helicopter was also sized for an alternate mission, composed of three 400 nm segments (takeoff, climb, cruise at 30k, descent, and landing; with one reserve segment), instead of a single 1200 nm segment. Table 8 shows the aircraft designed for the alternate mission. The additional climb and descent time in the 3x400 mission resulted in heavier aircraft carrying more fuel. Thus, the aircraft required longer and wider rotor blades.

To explore the influence of the design condition on performance, the performance optimization and aircraft sizing were performed for the following alternate design cruise conditions:

a) 30k ISA and 350 knots
b) 20k ISA and 350 knots
c) 20k ISA and 250 knots
d) 10k ISA and 250 knots
e) 5k ISA+20^{o}C and 250 knots

In this study, designs were developed for both tandem main rotors and a single main rotor configurations. The comprehensive analysis was used to optimize the rotor performance. The comprehensive analysis results were used to estimate aircraft L/D=WV/P as a function of flight speed, as shown in Fig. 18. The performance calculation used the disk loading of 15 lb/ft^2 and total drag $D/q/(W/1000)^{2/3}$ = 1.9. The number of blades was increased to six to obtain a reasonable chord length. The optimum twist was 0 deg inboard (0.0R to 0.5R) and -12 deg outboard (0.5R to 1.0R), same as the baseline, and the taper was 0.8 (tip/root chord). The optimum tip speed was found to be M_{at} = 0.60 for 5k ISA+20^{o}C and 250 knots, M_{at} = 0.65 for 20k ISA and 250 knots and for 10k ISA and 250 knots, and M_{at} = 0.85 for 30k ISA and 350 knots and for 20k ISA and 350 knots. The rotor/rotor interference resulted in a small reduction in aircraft L/D for the tandem configuration compared to the single main rotor. The efficiency improves as altitude increases because the lower density makes it more efficient for the wing to generate the required lift.

Conclusions

A heavy lift slowed-rotor compound helicopter was designed as a part of the NASA Heavy Lift Rotorcraft Systems Investigation. The vehicle is required to carry 120 passengers over a range of 1200 nautical miles and cruise at an altitude of 30,000 ft at 350 knots. The basic size of the helicopter was determined by the U.S. Army Aeroflightdynamics Directorate's design code RC. Then performance optimization and loads and stability analyses were conducted with the comprehensive rotorcraft analysis CAMRAD II. Blade structural design (blade inertial and structural properties) was carried out using the loading condition from CAMRAD II. Performance optimization was conducted to find the optimum twist, collective, tip speed, and taper using the comprehensive analysis. The final design showed an efficient hover and cruise speed capability (hover figure of merit of 0.73 and aircraft lift-to-drag ratio of 10.14), without any stability issues either in hover or in high advance ratio forward flight.

Designs were also developed for alternate missions to explore the influence of the design condition on performance. In this study, both tandem main rotors and a single main rotor configurations were developed. The rotor/rotor interference resulted in a small reduction in aircraft L/D for the tandem configuration compared to the single main rotor. The efficiency improves as altitude increases because the lower density makes it more efficient for the wing to generate the required lift.

References

[1] Johnson, W., Yamauchi, G. K., and Watts, M. E., "Design and Technology Requirements for Civil Heavy Lift Rotorcraft," Proceedings of the American Helicopter Society Vertical Lift Aircraft Design Conference, San Francisco, CA, January 2006.

[2] Preston, J., and Peyran, R., "Linking a Solid-Modeling Capability with a Conceptual Rotorcraft Sizing Code," Proceedings of the American Helicopter Society Vertical Lift Aircraft Design Conference, San Francisco, CA, January 2000.

[3] Johnson, W., "Technology Drivers in the Development of CAMRAD II," Proceedings of the American Helicopter Society Aeromechanics Specialist Meeting, San Francisco, CA, January 1994.

[4] Zhang, J., and Smith, E., "Design Methodology and Analysis of Composite Blades for a Low Weight Rotor," Proceedings of the American Helicopter Society Vertical Lift Aircraft Design Conference, San Francisco, CA, January 2006.

[5] Yeo, H., Bousman, W. G., and Johnson, W., "Performance Analysis of a Utility Helicopter with Standard and Advanced Rotor," *Journal of the American Helicopter Society*, Vol. 49, No. 3, July 2004.

[6] Yeo, H., and Johnson, W., "Assessment of Comprehensive Analysis Calculation of Airloads on Helicopter Rotors," *Journal of Aircraft*, Vol. 42, No. 5, September-October 2005.

[7] Yeo, H., and Johnson, W., "Comparison of Rotor Structural Loads Calculated Using Comprehensive Analysis," Proceedings of the 31st European Rotorcraft Forum, Florence, Italy, September 2005.

[8] Johnson, W., Yamauchi, G. K., and Watts, M. E., "NASA Heavy Lift Rotorcraft Systems Investigation," NASA TP-2005-213467, September 2005 (in publication).

[9] Handschuh, R. F., "Current Research Activities in Drive System Technology in Support of the NASA Rotorcraft Program," Proceedings of the American Helicopter Society Vertical Lift Aircraft Design Conference, San Francisco, CA, January 2006.

Table 1 Rotorcraft notional vehicle 15-year capabilities.

Payload	120 passengers
Cruise speed	M = 0.60 (350 knots) at 30,000 ft
Range	1200 nm
Operations	Automated single-pilot CAT IIIC SNI for heavy lift

Table 2 Rotorcraft vehicle sector 15-year technology goals.

Hover efficiency, W/P	6
Efficient cruise, L/D	12
Empty weight fraction	0.41
Community noise	SOA-14 EPNdb
Flight control	Automated single-pilot CAT IIIC SNI
Advanced engine SFC	SOA-10%
Advanced engine SHP/W	SOA*120%
Cabin noise and vibration	77dBA & 0.05g

Table 3 Design mission.

1200 nm range, 120 passengers	
Cruise at 350 knots and 30,000 ft (min 22,000 ft, for icing)	
Design mission	
Idle 5 min	
Takeoff + 1 min HOGE	5k ISA+20^{O}C
[convert]	
Climb at V_{br} (0k ISA to 30k ISA, distance part of range)	
Cruise at 350 knots, for 1200 nm range	30k ISA
Reserve: 30 min + 30 nm at V_{br}	30k ISA
Descent at V_{br} (no range credit)	
[convert]	
1 min HOGE + Landing	5k ISA+20^{O}C
Idle 5 min	
Design power	
Hover: 95% MRP, 5k ISA+20^{O}C	
Cruise: 100% MCP, 30k ISA	
One engine inoperative (OEI)	
at 5k ISA+20^{O}C, 133% (OEI MCP) greater than 90% (HOGE P_{req})	
at 22k ISA, (OEI MCP) greater than (P_{req} at V_{br})	
4 engines	

Table 4 Critical design conditions for aeromechanics analysis.

Blade stability
Thrust sweep in hover (SLS), to rotor stall
Level flight speed sweep (30k ISA), to maximum power
Performance
Thrust sweep in hover (5k ISA+20^{o}C), for power and figure of merit
Speed sweep in high speed forward flight (30k ISA) for power and efficiency
Loads (blade, hub, control), deflection, and vibration
Load factor sweep at 80 knots (SLS), to 1.5g
Level flight speed sweep (30k ISA), to maximum power

Table 5 Advanced technology estimates.

Hover C_W/σ, (5k ISA+20^{o}C)		0.141
Hover download		5.7%
Tip speed, hover	ft/sec	650
Tip speed, cruise	ft/sec	205
Cruise speed, 30k	knots	350
Drag, $(D/q)/(W/1000)^{2/3}$	ft^2	1.9
Wing loading	lb/ft^2	80

Table 6 Cruise drag buildup.

Wing D/q	15.84
Area	1735
C_D	.0091
Body D/q	12.42
S_{wet}	3650
C_f	.0021
Interference	4.86
Horizontal tail D/q	1.92
Area	217
Pylon D/q	9.39
Hub D/q	10.72
Hub D/q/(W/1000)$^{(2/3)}$	.40
Total D/q	50.28
D/q/(W/1000)$^{(2/3)}$	1.88

Table 7 Characteristics of the heavy lift slowed-rotor tandem compound helicopter design.

Mission GW (lb)	138,764
Engines (hp)	4x9684
Mission fuel (lb)	17,902
Rotor diameter (ft)	76.7
Disk loading W/A (lb/ft^2)	15
C_W/σ (geom, 5k ISA+20^{o}C)	0.133
C_W/σ (T-wt, 5k ISA+20^{o}C)	0.141
Tip speed (ft/sec)	650/205
maximum M_{at}	0.80
Solidity	0.1321
Number of blades	4
Chord (75%R, ft)	3.98
Aspect ratio	9.6
Taper ratio	0.8
Drag D/q (ft^2)	50.3
(D/q)/(W/1000)$^{2/3}$	1.9
Wing loading (lb/ft^2)	80
Area (ft^2)	1735
Span (ft)	144
Aspect ratio	12.0
Cruise power (hp)	14,724
Cruise L/D=WV/P	10.14

Table 8 Designs for alternate (three 400 nm segments) mission.

Gross weight (lb)	155,540
Engine power (hp)	4x10,819
Mission fuel (lb)	24,894
Rotor diameter (ft)	81.2
Disk loading W/A (lb/ft^2)	15
C_W/σ (T-wt, 5k ISA+20^{o}C)	0.141
Number of blades	4
Chord (75%R, ft)	4.22
Wing loading (lb/ft^2)	80
Drag D/q (ft^2)	55.0

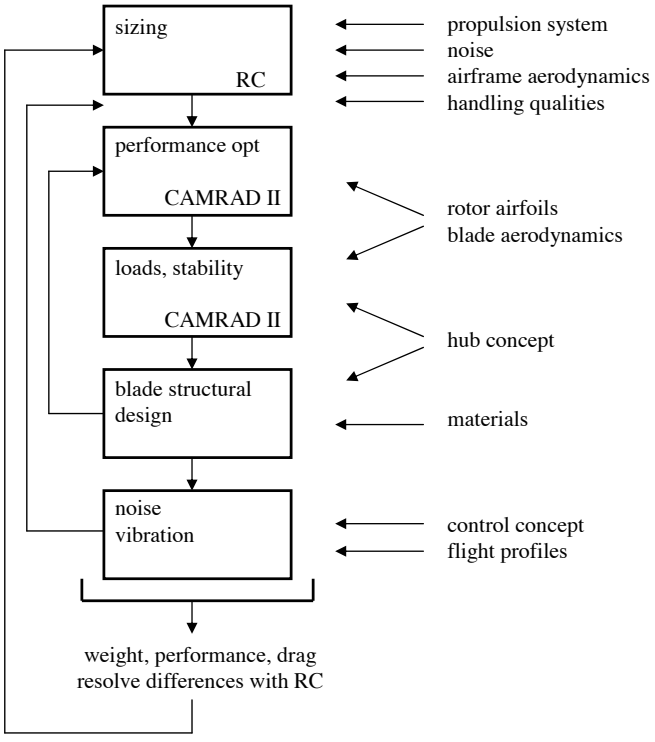

Fig. 1 Design iteration process.

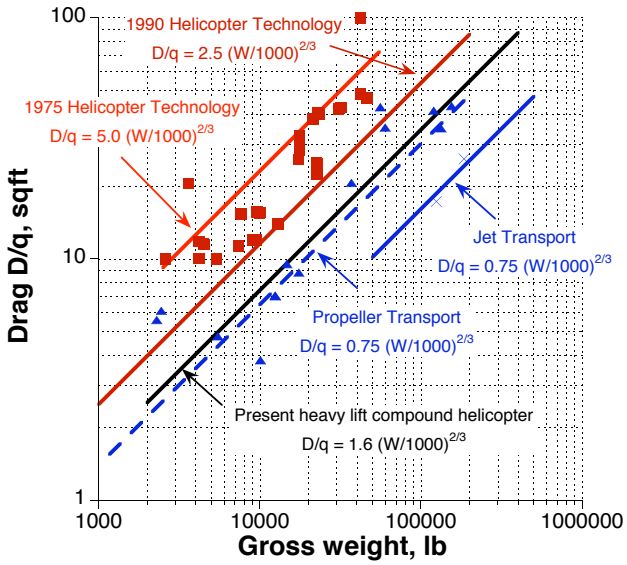

Fig. 2 Aircraft drag trends (courtesy F. D. Harris).

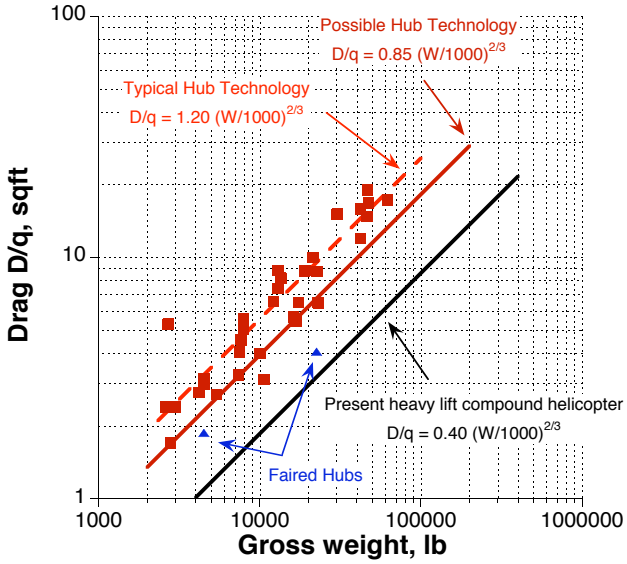

Fig. 3 Rotor hub drag trends (courtesy F. D. Harris).

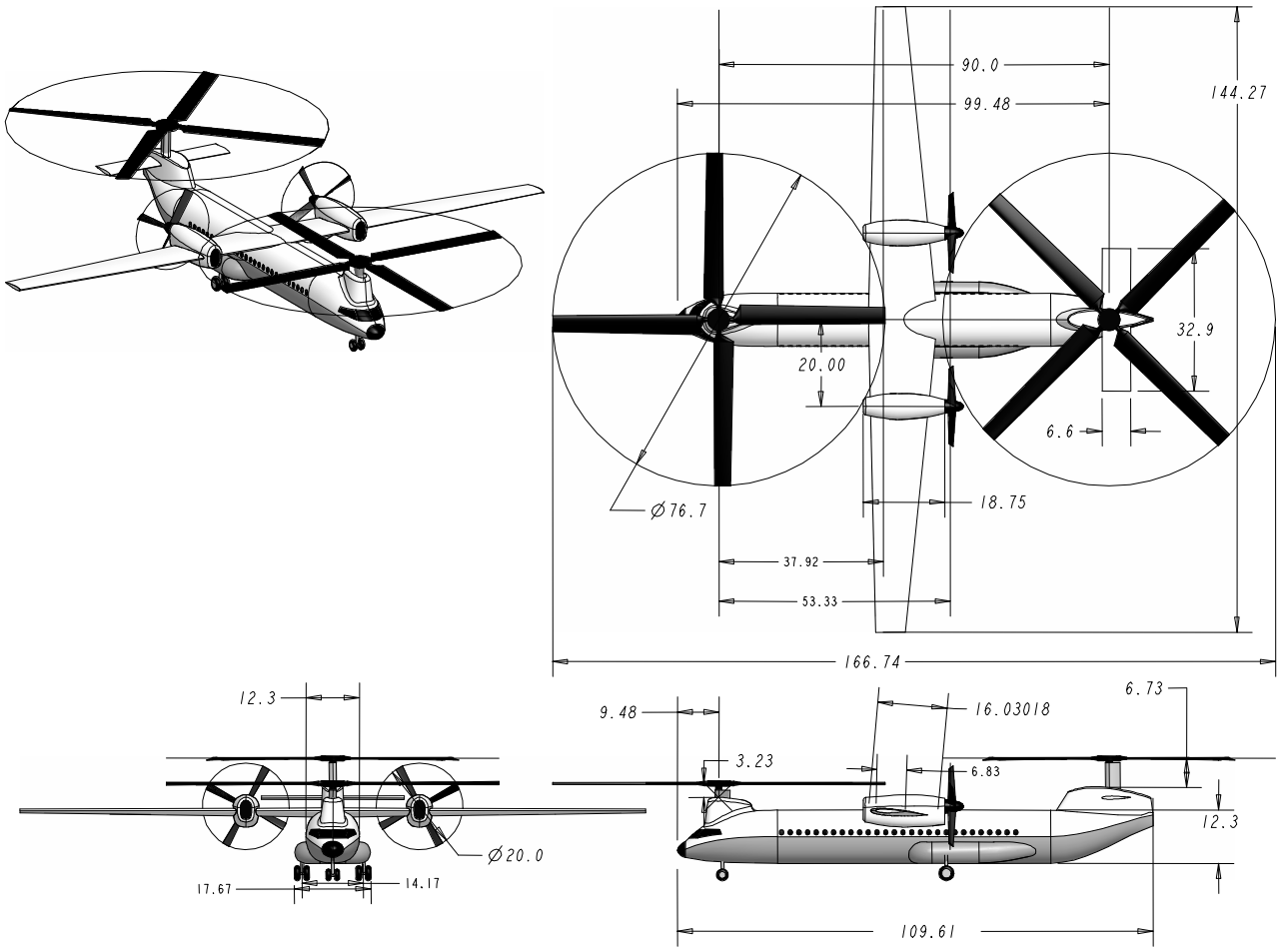

Fig. 4 Three-view of the heavy lift slowed-rotor tandem compound helicopter.

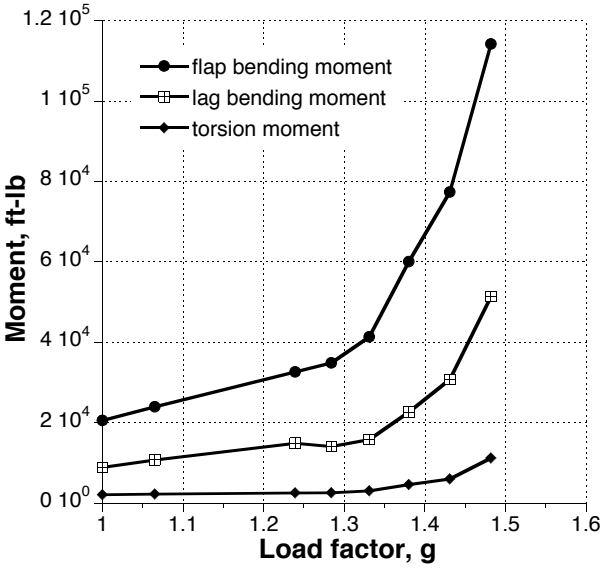

Fig. 5 Oscillatory blade structural loads at 50%R for load factor sweep.

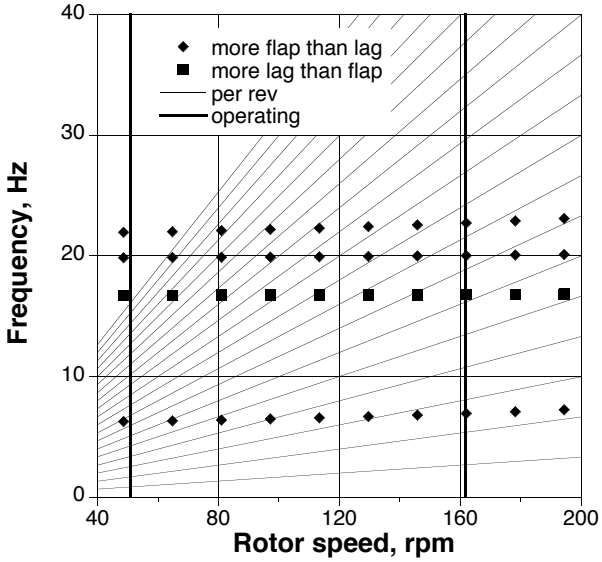

Fig. 7 Blade frequencies (collective = 10 deg).

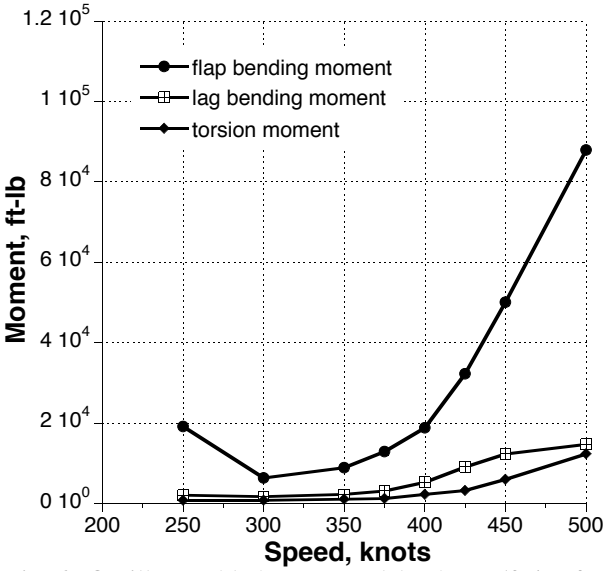

Fig. 6 Oscillatory blade structural loads at 50%R for level flight.

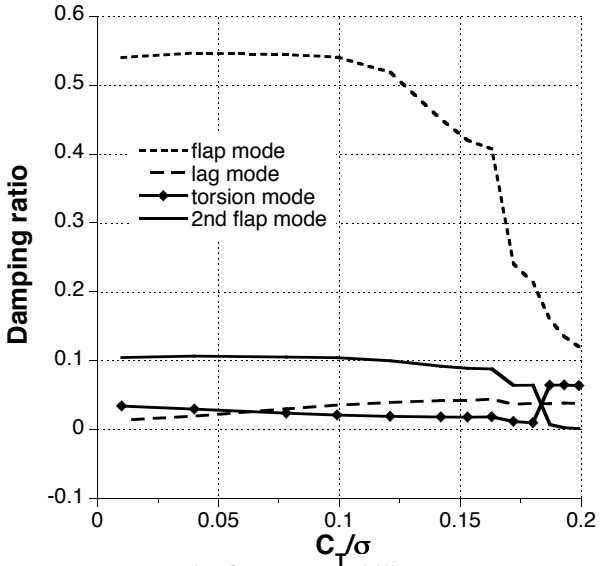

Fig. 8 Hover stability.

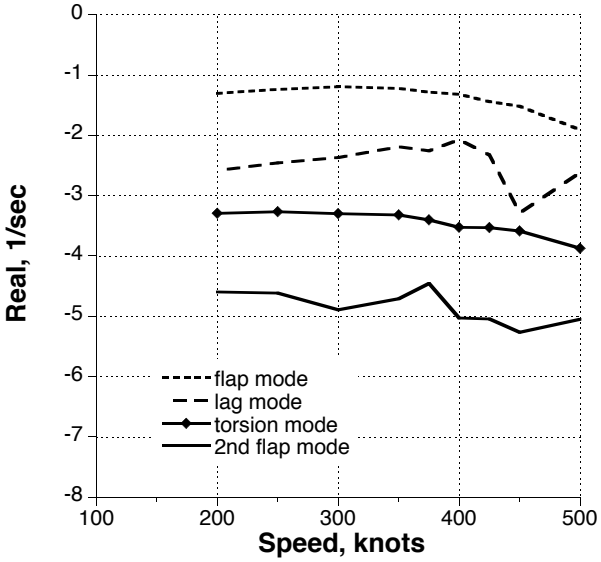

Fig. 9 Cruise stability.

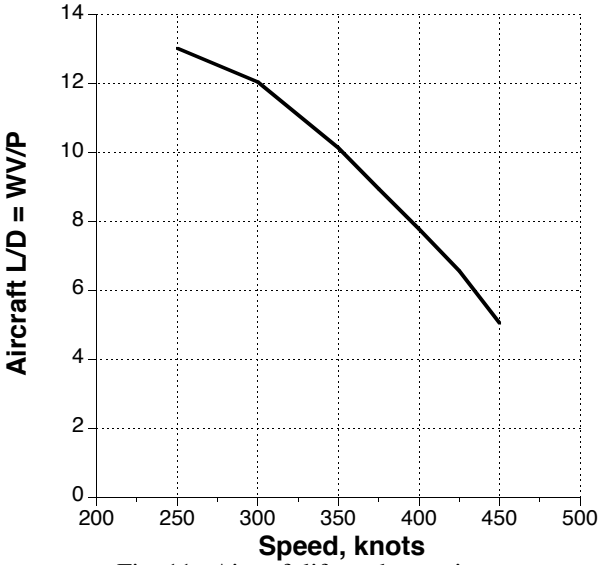

Fig. 11 Aircraft lift-to-drag ratio.

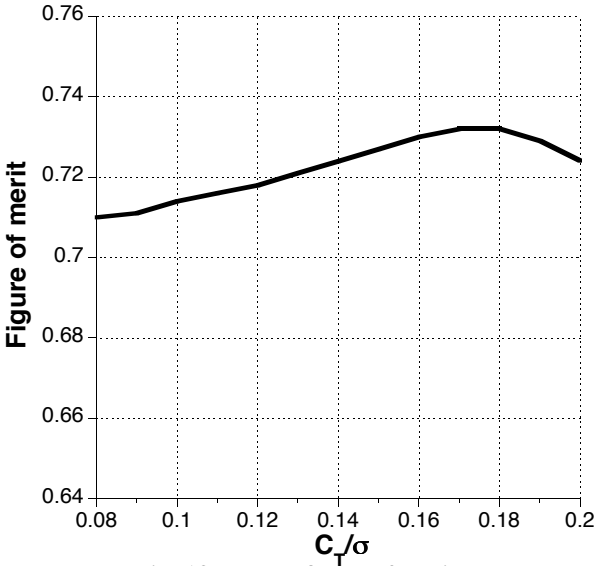

Fig. 10 Hover figure of merit.

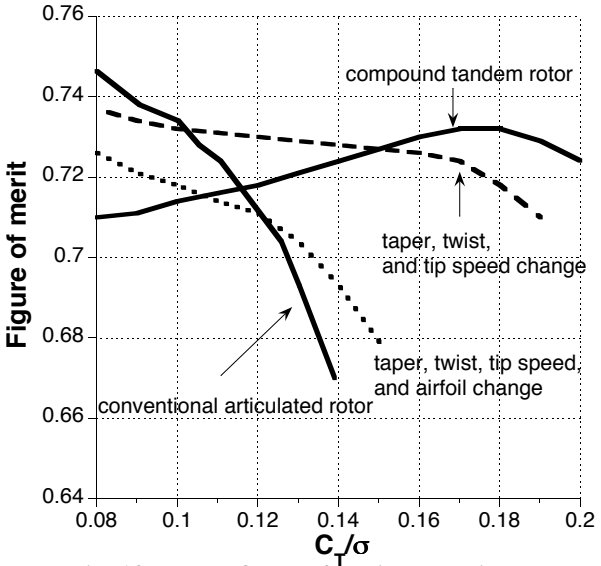

Fig. 12 Hover figure of merit comparison.

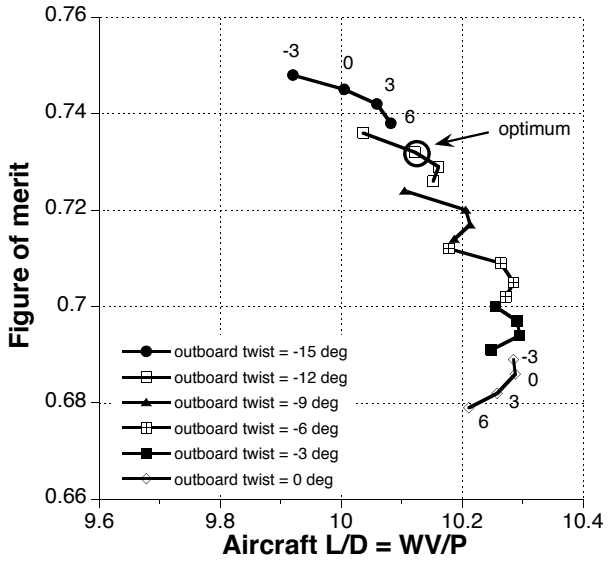

Fig. 13 Twist optimization (inboard twist = -3, 0, 3, 6 deg).

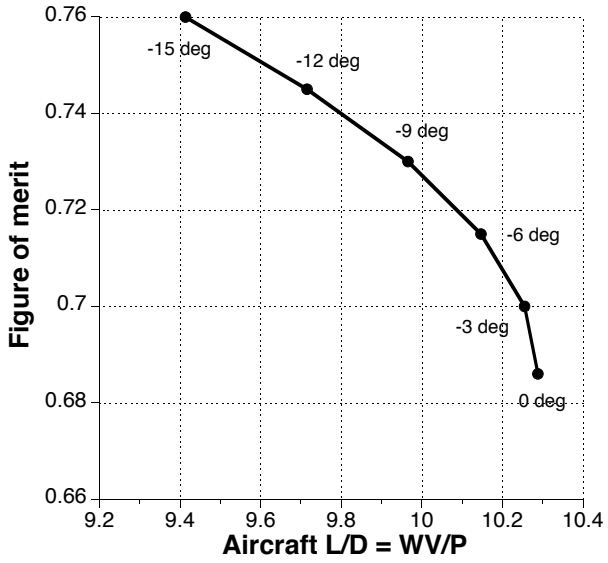

Fig. 14 Performance with linear twist.

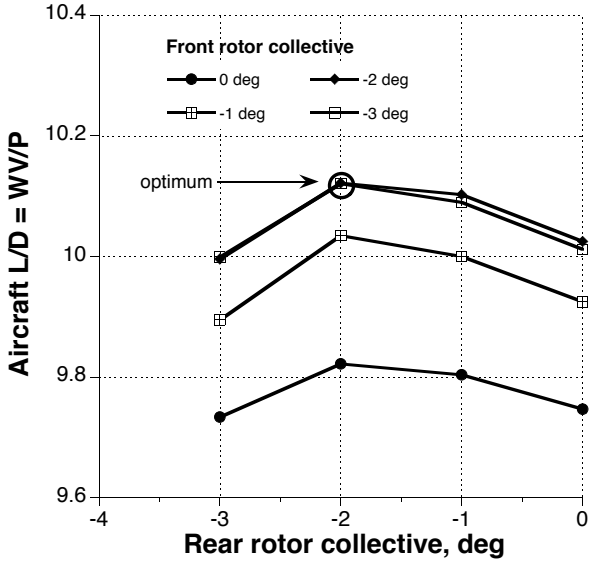

(a) Aircraft L/D

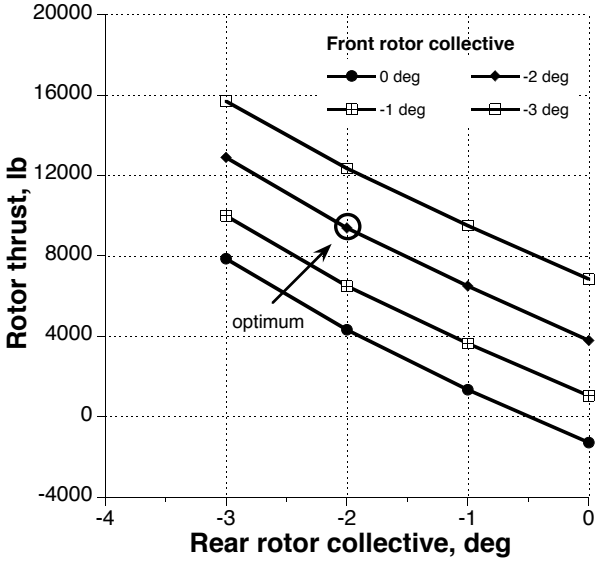

(b) Rotor thrust

Fig. 15 Collective optimization.

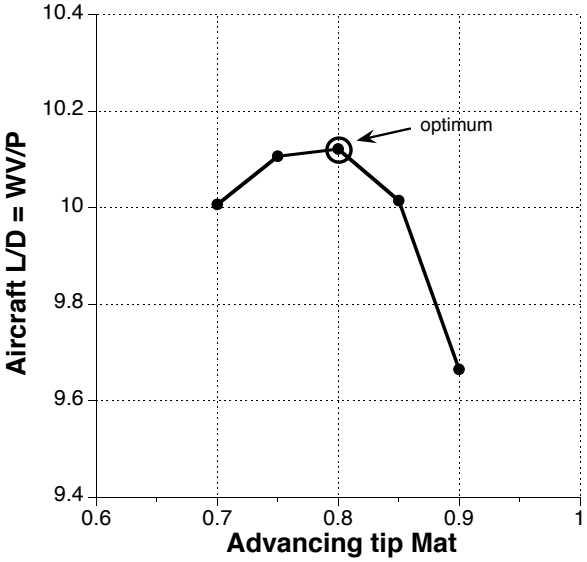

Fig. 16 Tip speed optimization.

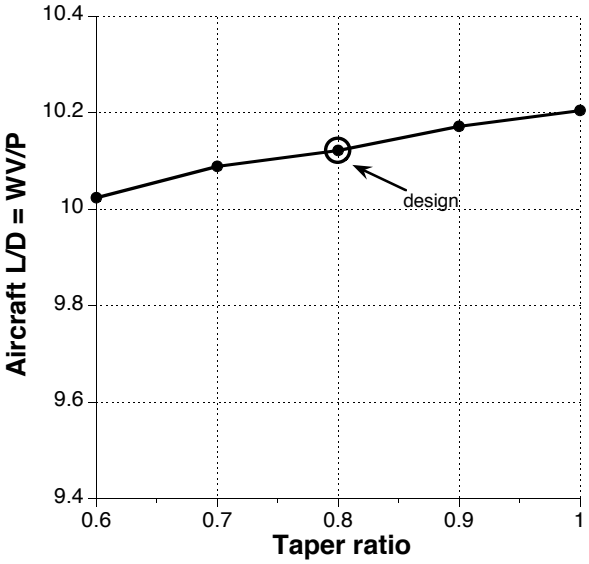

Fig. 17 Taper optimization.

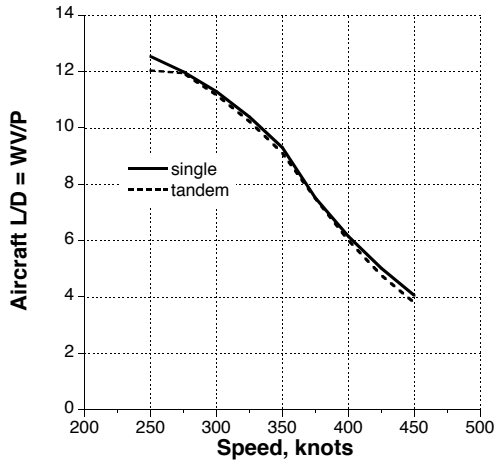

(a) 30k ISA and 350 knots

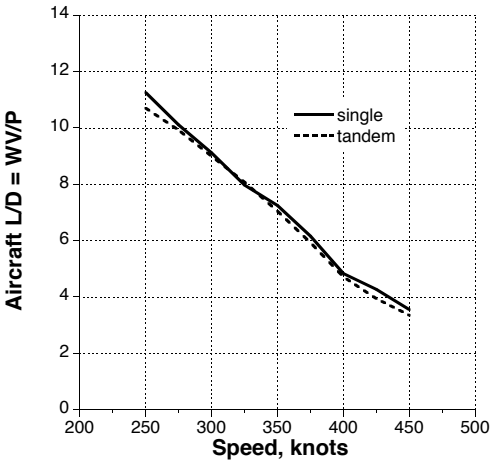

(b) 20k ISA and 350 knots

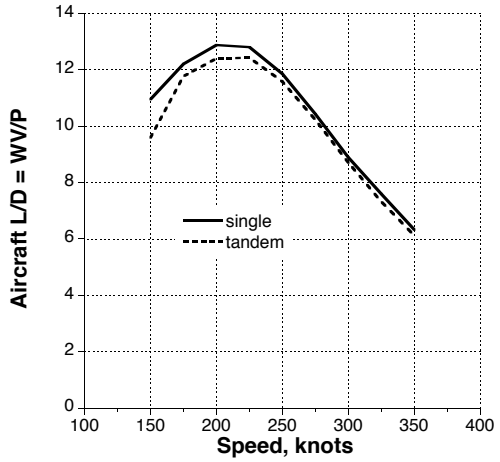

(c) 20k ISA and 250 knots

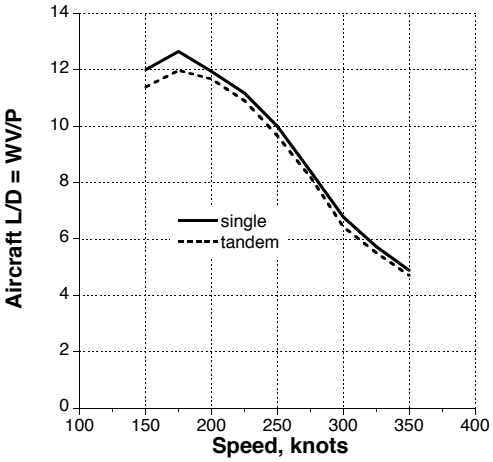

(d) 10k ISA and 250 knots

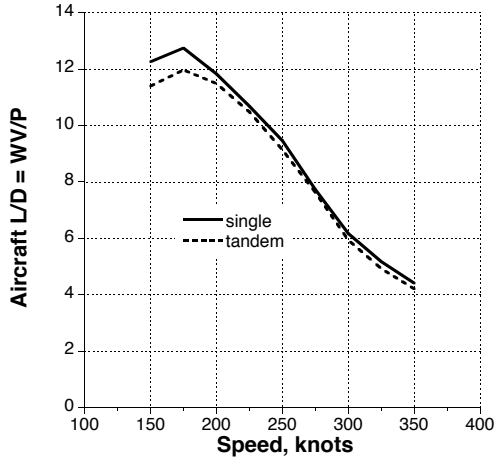

(e) 5k ISA+20^{o}C and 250 knots

Fig. 18 Aircraft L/D for different design conditions.